

## **GLOBAL DAMAGE IDENTIFICATION BASED ON VIBRATION SIGNATURES APPLIED TO MASONRY STRUCTURES**

LUÍS F. RAMOS<sup>†</sup>, PAULO B. LOURENÇO<sup>†</sup>, GUIDO DE ROECK<sup>\*</sup>,  
ALFREDO CAMPOS-COSTA<sup>\*\*</sup>

<sup>†</sup>University of Minho, ISISE, Portugal, e-mail: lramos@civil.uminho.pt

<sup>\*</sup>Catholic University of Leuven, Department Civil Engineering, Belgium

<sup>\*\*</sup>Laboratório Nacional de Engenharia Civil, Portugal

### **SUMMARY**

The present paper aims at damage assessment of masonry structures in an early stage. Two replicates of historical constructions were built in virgin state, one arch with 1.5 m span and one shear wall of 1 m<sup>2</sup>. Afterwards, progressive damage was applied and sequential modal identification analysis was performed in each damage stage, aiming at finding adequate relations between changes in dynamical behaviour and internal crack growth. During the dynamic tests, accelerations and strains were recorded in many points of the replicates. Comparisons between different techniques based on vibrations measurements were made to evaluate which methods are the most suitable for identifying damage in masonry constructions.

### **INTRODUCTION**

Preservation of the architectural heritage is considered a fundamental issue in the cultural life of modern societies. Modern requirements for an intervention include reversibility, unobtrusiveness, minimum repair and respect of the original construction, as well the obvious functional and structural requirements.

In the process of preservation of ancient masonry structures, damage evaluation and monitoring procedures are particularly attractive, due to the modern context of minimum repair and observational methods, with iterative and step-by-step approaches. High-priority issues related to damage assessment and monitoring include global non-contact inspection techniques, improved sensor technology, data management, diagnostics (decision making and simulation), improved global dynamic (modal) analysis, self-diagnosing / self-healing materials, and improved prediction of early degradation. This paper focus on improved global (dynamic) modal analysis for damage detection.

### **DAMAGE IDENTIFICATION PROCESS**

The present paper deals with the problem of damage identification by using Global and Local damage identification techniques. It is advantageous to have two categories of damage assessment methods: (a) the vibration based damage identification methods, currently defined as Global methods, because they do not give sufficiently accurate information about the extent of the damage, but they can identify its presence and define its precise location (e.g. Chang et al., 2003); and (b) the methods based on visual inspections or experimental tests, such as

acoustic or ultrasonic methods, magnetic field methods, radiograph and thermal field methods (e.g. Doherty, 1987), also called as Local methods. The latter need a preceding global approach (Global methods) to detect and localize the damage, and then, if the possible location of damage is accessible in the structure, they can describe the damage in an accurate way.

Damage on masonry structures mainly relates to cracks, foundation settlements, material degradation and displacements. When cracks occur, generally they are localized, splitting the structures in macro-blocks. Dynamic based methods to assess the damage are an attractive tool for this type of structure due to the present requirements of unobtrusiveness, minimum physical intervention and respect of the original construction. The assumption that damage can be linked to a decrease of stiffness seems to be reasonable for this type of structure.

Many methods are presented in the literature, see Doebling et al. (1996), for damage identification based on vibration signatures but there are only a few papers on the application to masonry structures. An important task before damage can be identified from vibration characteristics is the study and subsequent elimination of the environmental effects (Peeters, 2000), which for masonry structures can have significant importance (Ramos, et al., 2007).

### Proposed Methodology

A group of damage methods has been selected from the literature. In one hand, it is intended to study the applicability of existing methods to the masonry structures, and, in another hand, it is aimed to have a wide view of the problem (different results are provided by different methods), assisting in the conclusions related to damage identification. If significant damage is present in the structure, the results provided from different methods would converge in a unique conclusion, giving more confidence to the analyzer. The selected methods together with the required modal information are presented in Table 1 (see Doebling et al., 1996, for the complete description of each method).

Table 1. Selected damage identification methods

Method	Type	Expected Identification Level	Comparison to a Ref. Scenario	Modal Information				
				$\omega$	$\varphi$	$\varphi''$	$\phi$	$\phi''$
Unified Significance Indicator (USI)	Non-Model Based	Level 1	Yes	•				
COMAC		Level 2	Yes		○	○	○	○
Parameter Method (PM)		Level 2	Yes	•	○	○	○	○
Mode Shape Curvature Method (MSCM)		Level 2	Yes			○		○
Damage Index Method (DIM)		Level 2	Yes			○		○
Sum of the Curvature Errors method (SCE)		Level 2	Yes			○		○
Change Flexibility Matrix method (CFM)	Model Based	Level 2 and 3	Yes	•			•	○
FE Model Updating method (FEMU)		Level 2 and 3	No	○	○	○	○	○

○ – Optional modal quantities; • – Compulsory modal quantities ; Level 1 – Detection ; Level 2 – Localization ; Level 3 – Quantification

All methods have one common aspect; they all use spatial modal information of the structure, through the mass scaled or non-scaled mode shapes  $\phi$  and  $\varphi$ , respectively (or/and through the mass scaled or non-scaled curvatures mode shapes  $\phi''$  and  $\varphi''$ , respectively).

The methods were applied to the experimental models, where progressive and controlled damage scenarios were imposed. From the point of view of the applicability of dynamic based identification methods to masonry structures, the methodology would be successful if the detection (Level 1), the localization (Level 2) and the assessment (Level 3) will be attained with these methods.

The global and local approach should be considered as complementary tasks. For the case of historical constructions these two approaches seem to be suitable, since they are non-destructive procedures to evaluate health conditions.

## DESCRIPTION OF THE MODELS AND EXPERIMENTAL TEST

One replicate of ancient masonry arches and one replicate of a shear wall were built in the laboratory. The arch was built with clay bricks with  $100 \times 50 \times 25 \text{ mm}^3$  and the wall with clay bricks with  $210 \times 105 \times 55 \text{ mm}^3$ . The bricks were handmade in the Northern area of Portugal. The clay brick, with low compression strength, and the Mapei® mortar, with poor mechanical properties, used for the joints tries to be representative of the materials used in the historical constructions. Figure 1 shows some images of the replicates. The arch has a semicircular shape with a radius of 0.77 m, a span of 1.50 m, a width of 0.45 m, and a thickness of 0.05 m, and rests in two concrete abutments fixed to the ground floor with bolts. The wall has a length equal to 1.08 m, a height equal to 1.10 m, and a thickness equal to 0.105 m, exactly the bricks thickness. The wall rests in a steel beam fixed to the ground floor with bolts. All the tests were carried out after 60 days of the specimens' construction.

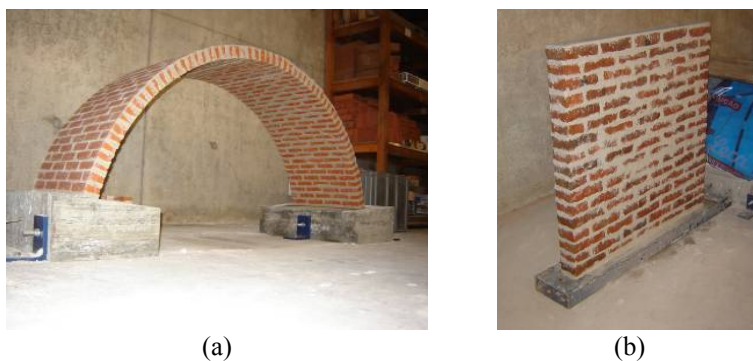


Figure 1. Masonry replicates: (a) arch model; and (b) wall model

### Static Tests

Progressive and controlled damage were applied by static increasing loads to reach multiple damage levels (several cracks). The loads were applied and removed with linear branches for all the levels. Between each stage (damage scenario), modal identification analysis using output-only (ambient or natural vibration) techniques were performed, where the ambient temperature and humidity were also recorded, to evaluate possible environmental effects on the dynamic response.

For the case of the arch, eight Damage Scenarios (from DS<sub>I</sub> to DS<sub>VIII</sub>) were induced. Figure 2a shows the load application point and the resulted four cracks ( $c_1$ ,  $c_2$ ,  $c_3$  and  $c_4$ ). Figure 2b shows the response of the model during the subsequent static tests, where it is possible to visualize the probable occurrence of the cracks and the stiffness decrease after each damage scenario. Figure 2c presents one of four cracks found in the arch. It should be stressed that the maximum remaining crack opening after the applied loads was 0.05 mm and the maximum crack depth in the loading branch was 30 mm for crack  $c_1$  (more than half of the arch thickness).

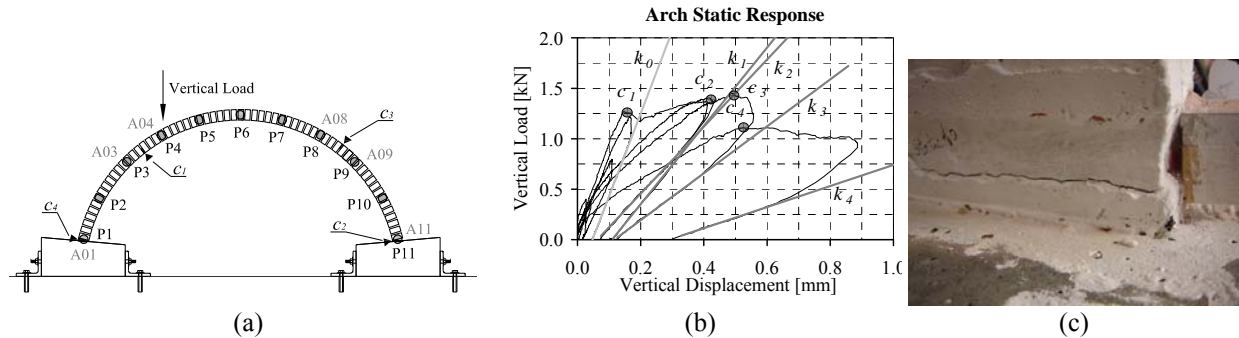


Figure 2. Arch static tests: (a) crack locations and sensor positions; (b) static structural response; and (c) crack  $c_2$  in the intrados

For the case of the wall model, fourteen DS were produced, divided in three series of tests. The static forces were applied to produce constant compressive stresses and varying shear stresses. Figure 3 presents for the last series of tests the static response and the final crack pattern. Three cracks occurred ( $c_1$ ,  $c_2$  and  $c_3$ ). The maximum openings were equal to 2.00 mm for crack  $c_1$ , 0.10 mm for crack  $c_2$  and 1.20 mm for the shear crack  $c_3$ .

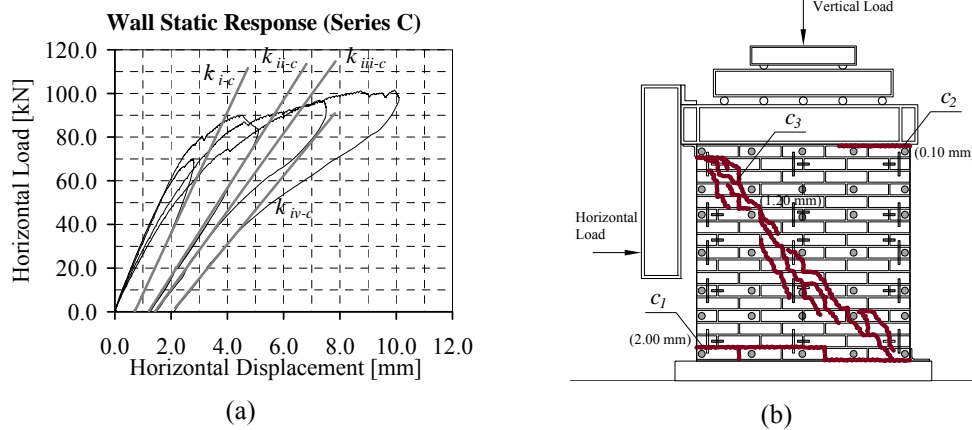


Figure 3. Wall static tests for the last test series: (a) static structural response; and (b) the final crack pattern

## Dynamic Tests

For the arch model and in order to have a clear definition of the modal displacements, it was decided to make the measurements in 11 points uniformly distributed along the arch. The 11 points were materialized along two lines at the specimen sides for the accelerometers and along the specimen centre line for the strain gauges. In total, 44 different directions for accelerations (each side, in radial and tangential directions) and 22 strain points (intrados and extrados, in tangential direction) were measured. Figure 4 shows some images of the sensors location in the arch.

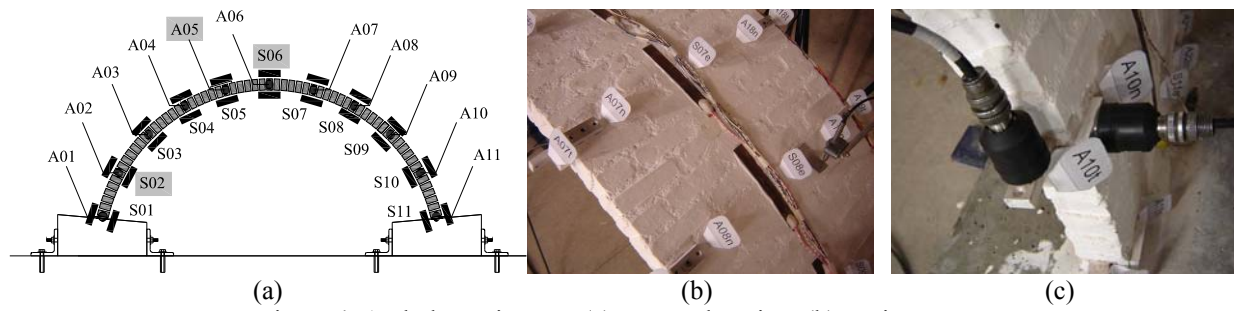


Figure 4. Arch dynamic tests: (a) sensors location; (b) strain gauges; and (c) normal and tangential accelerations measurements

For the wall model, a regular grid of five vertical lines and seven horizontal lines was chosen for accelerometers and a net of three vertical lines and five horizontal lines was chosen for strain gauges. Figure 5 shows the location of the measuring points. The strains were measured in two directions,  $x$  and  $z$ .

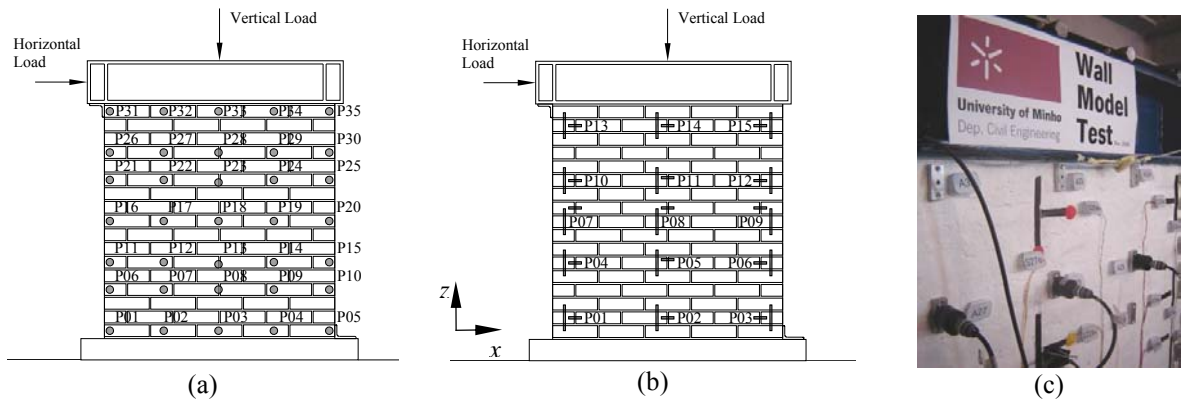


Figure 5. Wall dynamic tests: (a) net of accelerometers; (b) net of strain gauges; and (c) a detail of the sensors

In both specimens the accelerometers were bolted to aluminum plates that were directly glued to the specimens. The strain gauges in the arch model and the vertical strain gauges in the wall model have 12 cm of length and the horizontal strain gauges of the wall have 6 cm of length.

The dynamic tests were performed under two different type of excitations: ambient and random impacts introduced by an impact hammer. Only with random impact excitation it was possible to measure with accuracy the modal strains in the models.

## DAMAGE IDENTIFICATION ANALYSIS OF THE ARCH MODEL

The damage identification analysis was divided in three parts: the analysis of the global parameters changes, the analysis with non-model based methods and the analysis with the Finite Element model updating method. Here, only the first two analyses will be presented.

### Analysis of the Global Parameters

Table 2 presents the frequency results for the progressive damage scenarios and Figure 6a gives the relative variation of the frequencies. Observing the global frequency results, the modal properties of the masonry specimens seem sensitive to the damage progress. The resid-

ual values in the last scenario are between 78 and 95% of the reference values. These results seem promising, as other tests in the literature report smaller changes in frequencies values, see Doebling, et al. (1996). Another global parameter to study is the damping coefficient. Here, a significant increase of damping was observed after DS<sub>IV</sub>, see Figure 6b, where the average values for the damping coefficients using 6 and 7 mode shapes are presented.

Table 2. Frequency results for the arch model with ambient excitation

Damage Scenario	Mode 1			Mode 2			Mode 3			Mode 4		
	$\omega$ [Hz]	CV [%]	$\Delta\omega$ [Hz]	$\omega$ [Hz]	CV [%]	$\Delta\omega$ [Hz]	$\omega$ [Hz]	CV [%]	$\Delta\omega$ [Hz]	$\omega$ [Hz]	CV [%]	$\Delta\omega$ [Hz]
RS	35.59	0.57	–	67.30	0.69	–	72.11	0.53	–	125.74	0.52	–
DS <sub>I</sub>	35.55	0.44	–0.05	67.51	0.61	+0.21	71.80	0.27	–0.30	125.69	0.76	–0.05
DS <sub>II</sub>	35.55	0.34	–0.04	67.39	0.83	+0.09	71.83	0.74	–0.28	125.79	0.81	+0.05
DS <sub>III</sub>	35.42	0.44	–0.17	67.47	0.88	+0.17	71.66	0.66	–0.45	125.75	0.88	+0.01
DS <sub>IV</sub>	35.15	0.34	–0.44	67.11	0.66	–0.19	71.33	0.41	–0.78	126.01	0.43	+0.28
DS <sub>V</sub> <sup>†</sup>	33.72	0.48	–1.87	65.68	0.54	–1.62	69.36	0.43	–2.75	124.48	0.64	–1.25
DS <sub>VI</sub>	33.19	0.52	–2.40	64.91	0.79	–2.39	68.56	0.42	–3.55	123.58	0.56	–2.16
DS <sub>VII</sub>	31.49	0.69	–4.10	63.08	1.02	–4.22	65.72	0.52	–6.39	121.97	0.75	–3.77
DS <sub>VIII</sub>	28.09	1.11	–7.50	58.44	1.20	–8.86	62.61	0.74	–9.50	119.44	0.74	–6.30

<sup>†</sup> - Damage scenario where first visual the crack ( $c_I$ ) were localized

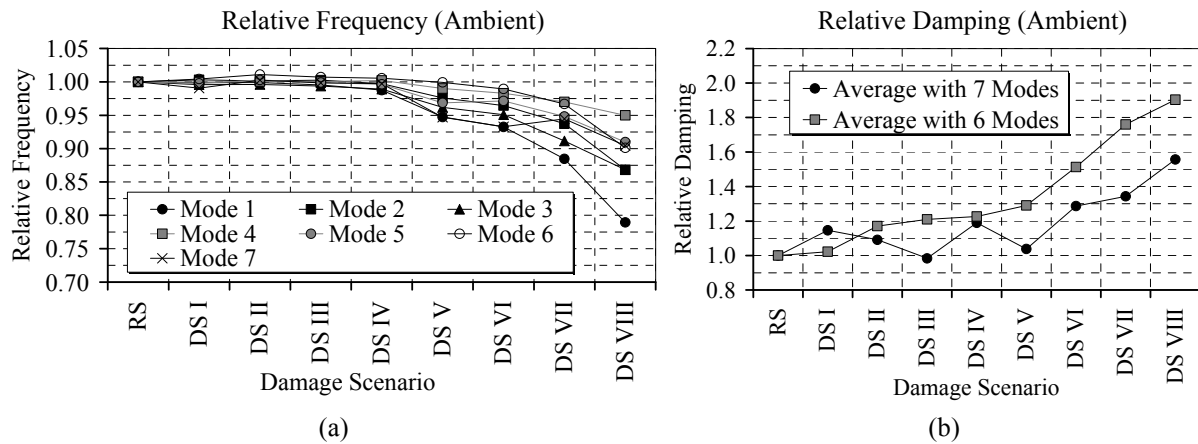


Figure 6. Dynamic global response of the arch model: (a) relative frequency variation; and (b) relative damping variation

### Analysis with Non-Model based Methods

Starting with the results from the USI method (see notation in Table 1), Figure 7 shows for both types of excitation the results for the comparisons with the Reference Scenario (RS) and the relative comparisons for each consecutive DS. In this analysis all the 7 estimated frequencies were considered. One conclusion emerged is the different values order before and after DS<sub>V</sub>, appointing that some significant change happened in this scenario. The following value, DS<sub>VI</sub>, is about the same order and in the last two a significant increasing is observed. These results indicate that when the USI is calculated for the several scenarios the detection of damage (Level 1) is possible and it confirms the analysis of the global parameters. For the case of no information about the modal information history, the detection of damage with USI might be difficult to predict, because no reference values in the undamaged condition are compared.

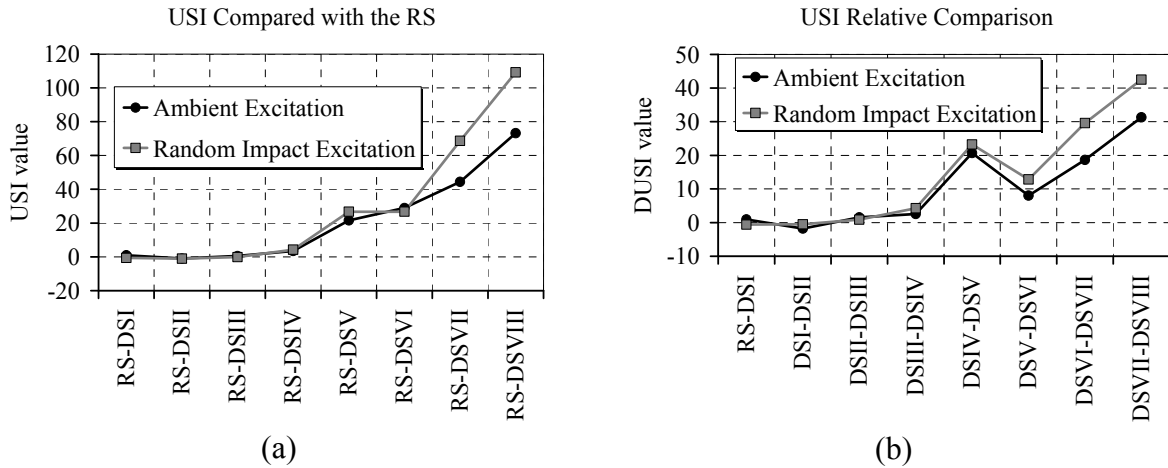


Figure 7. USI results for the arch model: (a) compared with the RS; and (b) relative comparison

Concerning the other non-model based methods (COMAC, PM, MSCM, DIM, SCE and CFM) some assumptions were made to increase the results quality. On each curvature mode shape the values close to zero were neglected in order to avoid any contamination in the results. In this way, only the significant values for curvatures and well estimated modes were compared, which makes the analysis more reliable. Therefore, the seeking of the damage location was based in the analysis of the results from the methods which gave consistent results, namely the MSCM, the DIM and the SCE. Figure 8 presents the final location results for three different comparisons.

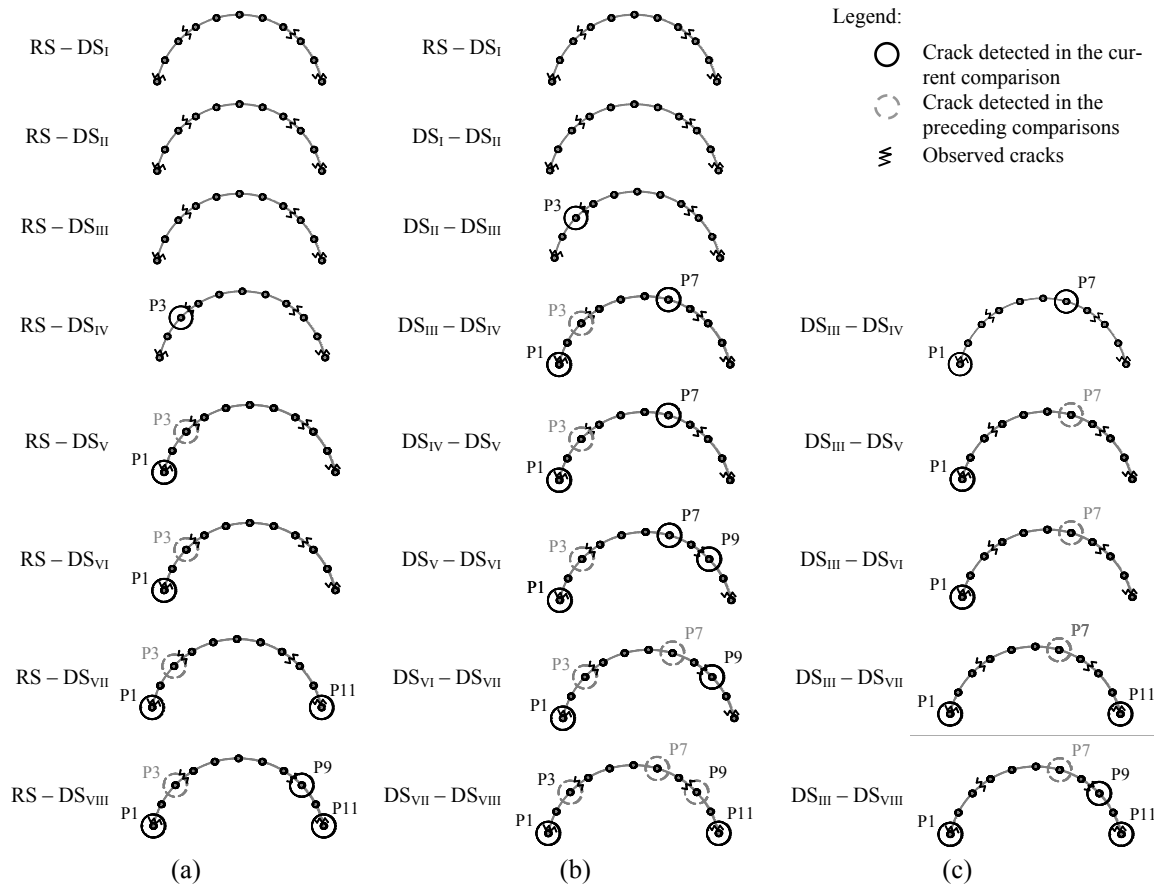


Figure 8. Damage location for the arch model: (a) comparison with the RS; (b) consecutive comparison with each DS; and (c) comparison with DS<sub>III</sub> as a new RS

From Figure 8 it was possible to conclude that the cracks could be localized (level 2) in the vicinity of the experimental cracks. Considering the above results, it seems that the combination of several damage methods based on experimental modal curvatures is a good methodology to detect and locate accurately and at an earlier stage the damage in the case of the masonry arch.

## DAMAGE IDENTIFICATION ANALYSIS OF THE WALL MODEL

The following Sections describe the damage identification analysis over the last test series of DS induced in the wall. The analysis was carried out taking into account the approach and the conclusions of the arch model analysis.

### Analysis of the Global Parameters

Analysing the frequency shifts presented in Table 3 there is an evidence of decreasing values after the observed crack. The significant frequency decrease, i.e. higher that  $2\sigma_\omega$  (given in a grey box), appended around the DS<sub>II</sub>, confirming the presence of damage (Level 1).

Table 3. Frequency results for the wall model with ambient excitation

Damage Scenario	Mode 1			Mode 2			Mode 3			Mode 4		
	$\omega$ [Hz]	$2\sigma_\omega$ [Hz]	$\Delta_\omega$ [Hz]	$\omega$ [Hz]	$2\sigma_\omega$ [Hz]	$\Delta_\omega$ [Hz]	$\omega$ [Hz]	$2\sigma_\omega$ [Hz]	$\Delta_\omega$ [Hz]	$\omega$ [Hz]	$2\sigma_\omega$ [Hz]	$\Delta_\omega$ [Hz]
RS	3.41	0.45	—	12.49	0.05	—	18.29	0.12	—	35.63	1.12	—
DS <sub>I</sub>	3.46	0.07	0.06	12.44	0.07	-0.05	18.24	0.07	-0.05	35.38	0.26	-0.25
DS <sub>II</sub> <sup>†</sup>	3.54	0.29	0.13	11.72	0.15	-0.77	17.56	0.18	-0.73	34.41	0.37	-1.22
DS <sub>III</sub>	2.99	0.05	-0.42	10.82	0.16	-1.67	16.76	0.19	-1.53	33.11	0.33	-2.52
DS <sub>IV</sub>	2.81	0.09	-0.60	9.27	0.20	-3.22	16.03	0.30	-2.26	32.52	2.78	-3.11

<sup>†</sup> - Damage scenario where visual the crack  $c_3$  were localized

Concerning the relative frequency values, Figure 9a show the progressive average frequency decrease with increasing damage. The residual value in the DS was equal to 0.84. Note that the term “relative frequency” has been used for the relation between the frequency in the DS and the original frequency in the RS. Figure 9b presents the relative average damping values, where one can conclude that there is a trend for the increasing damping through the DS, but the difficulties in the experimental estimation do not allow a complete conclusion of this fact.

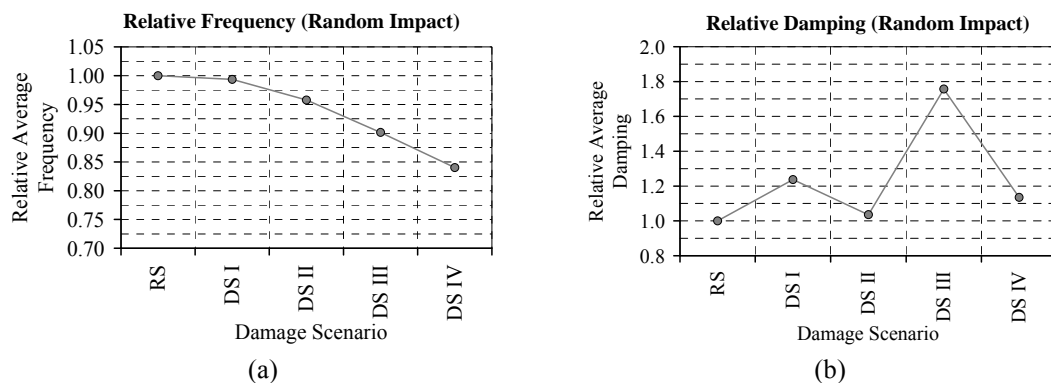


Figure 9. Dynamic global response of the wall model: (a) relative frequency variation; and (b) relative damping variation



## Analysis with Non-Model based Methods

Figure 10 presents the USI values for the comparison with the RS and the relative comparison between each consecutive DS. In both cases, there is an evident increasing of the USI values with the progressive damage, indicating that the severity of damage increase significantly with the static test.

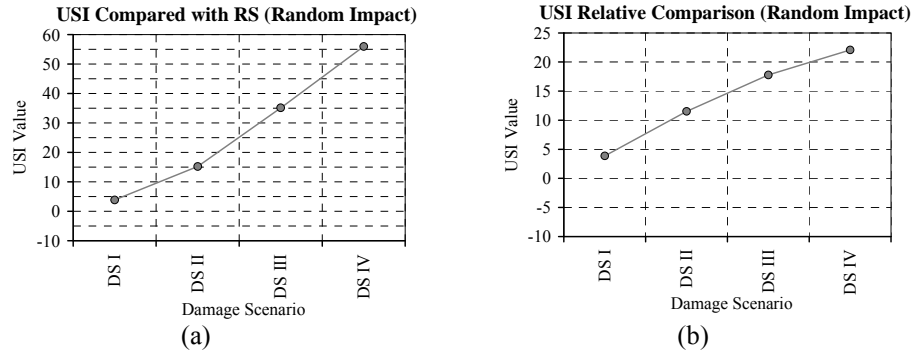


Figure 10. USI results for the wall model: (a) compared with the RS; and (b) relative comparison

As carried out in damage identification analysis of the arch model, for the application of non-model based methods the curvature mode shape values close to zero were neglected in order to avoid inaccurate results. Again, the seeking of the damage location was based in the methods which gave consistent results, namely the MSCM, the DIM and the SCE. Figure 11 shows the damage location for the case of the analysis with the RS.

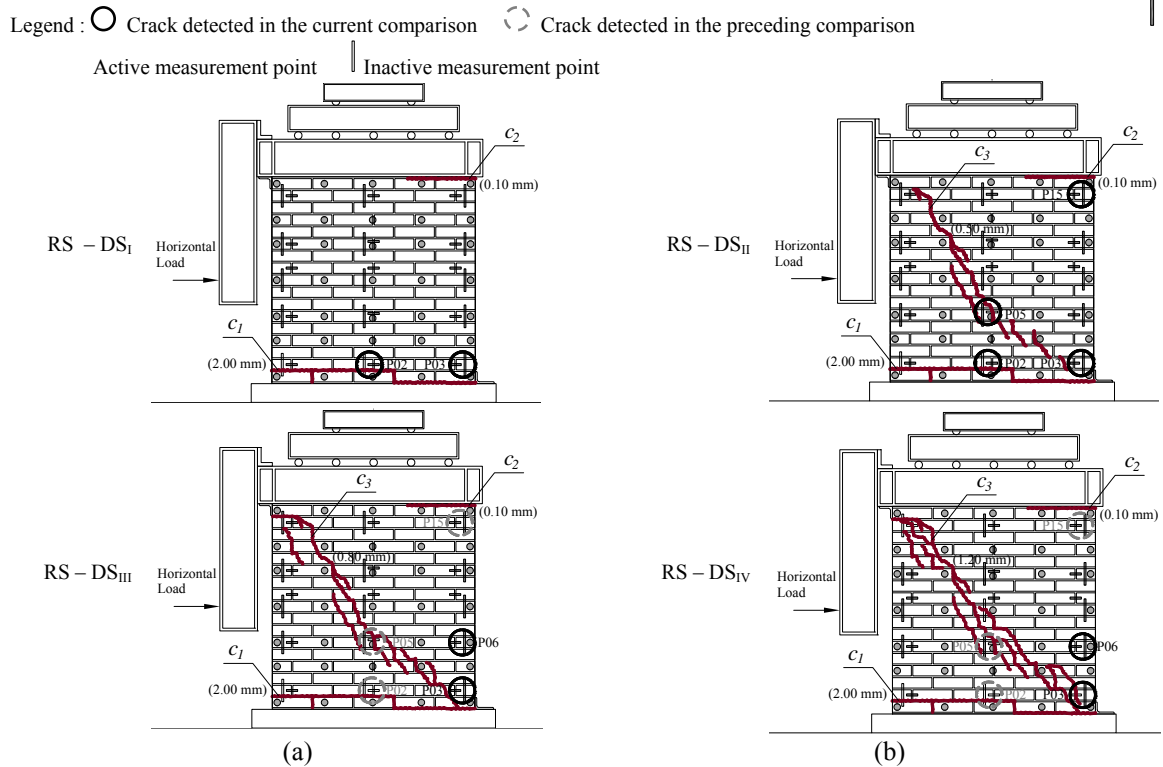


Figure 11. Damage location in the wall model

All the indicated damage locations are close to the observed cracks, including the localization of crack  $c_3$  in the same DS where it was experimentally possible to visualize first (DS<sub>II</sub>).

## CONCLUSIONS

This paper presents a damage analysis of two models studied in the laboratory. Controlled damage scenarios were applied and a damage analysis was performed with a selected group of methods by means of vibration signatures. The group of damage methods have a common feature: they all use spatial modal information, especially the modal curvatures, for damage identification.

The global results from the damage scenarios reveal that the modal properties of the masonry specimen are sensitive to the induced damage. In terms of frequency results, the frequency values significantly decrease at progressing damage, more than reported for other structures in the literature.

The selected group of damage methods demonstrate that damage can be successfully localized based on dynamic changes, especially if model curvatures are taking in to account. The cracks at an earlier stage were localised in the models.

If these observations are confirmed with real case studies, such as buildings, bridges or towers, the vibration based damage identification techniques applied to similar masonry constructions can be a useful tool in the conservation process of ancient masonry structures.

## REFERENCES

- Chang, P.C.; Flatau, A.; Liu, S.C. 2003. Review Paper: Health Monitoring of Civil Infrastructure, *Structural Health Monitoring*, Vol. 2 (3), pp. 257-267
- Doebbling, S.W.; Farrar, C.R.; Prime, M.B.; Shevitz, D. 1996. Damage identification and health monitoring of structural and mechanical systems from changes in their vibration characteristics: a literature review, Los Alamos National Laboratory, NM
- Doherty, J.E. 1987. Non-destructive Evaluation, *Handbook on Experimental Mechanics*, A.S. Kobavashi Edt., Society for Experimental Mechanics, Chapter 12
- Peeters, B. 2000. System Identification and Damage Detection in Civil Engineering, PhD Thesis, Catholic University of Leuven, Belgium
- Ramos, L.F.; Marques, L.; Lourenço, P.B.; Roeck, G.; Campos-Costa, A.; Roque, J. 2007. Monitoring Historical Masonry Structures with Operational Modal Analysis: Two Case Studies, 2nd International Operational Modal Analysis Conference, Copenhagen, April 30–May 2, 2007, vol. 1, pp. 161-168